

Casimir force driven ratchets

T. Emig

*Laboratoire de Physique Théorique et Modèles Statistiques,
CNRS UMR 8626, Université Paris-Sud, 91405 Orsay, France*

(Dated: May 10, 2018)

We explore the non-linear dynamics of two parallel periodically patterned metal surfaces that are coupled by the zero-point fluctuations of the electromagnetic field between them. The resulting Casimir force generates for asymmetric patterns with a time-periodically driven surface-to-surface distance a ratchet effect, allowing for directed lateral motion of the surfaces in sizeable parameter ranges. It is crucial to take into account inertia effects and hence chaotic dynamics which are described by Langevin dynamics. Multiple velocity reversals occur as a function of driving, mean surface distance, and effective damping. These transport properties are shown to be stable against weak ambient noise.

PACS numbers: 12.20.-m,05.45.-a,07.10.Cm

The observation of Casimir forces in increasingly small devices on sub-micron scales has generated great current interest in exploring the role of these forces for the development and optimization of micro- and nano-electromechanical systems [1, 2, 3]. These systems can serve as on-chip fully integrated sensors and actuators with a growing number of applications. It was pointed out that Casimir forces can make an important contribution to the principal cause of malfunctions of these devices in form of stiction that results in permanent adhesion of nearby surface elements [4]. This initiated interest in repulsive Casimir forces by modifying material properties as well as the geometry of the interacting components [5, 6].

A complementary strategy, which will be considered in this Letter, is to make actually good use of Casimir forces between metallic surfaces and employ them to actuate components of small devices without contact. We will demonstrate that this can be achieved by coupling two periodically structured (locally) parallel surfaces by the zero-point fluctuations of the electromagnetic field between them. The broken translation symmetry parallel to the surfaces results in a sideways force which has been predicted theoretically [7, 8] and observed experimentally between static surfaces [9]. If at least one of the surfaces is structured *asymmetrically* there is an additional breaking of reflection symmetry and the surfaces can in principle be set into relative lateral motion in the direction of broken symmetry. The energy for this transport has to be pumped into the system by external driving. This can be realized by setting the surfaces into relative oscillatory motion so that their normal distance is an unbiased periodic function of time. Since the sideways Casimir force decays exponentially with the normal distance [8], the surfaces experience an asymmetric periodic potential that varies strongly in time.

This scenario resembles so-called ratchet systems [10] that have been studied extensively during the last decade in the context of Brownian particles [11], molecular mo-

tors [12] and vortex physics in superconductors [13], to name a few recent examples. Most of the works on ratchets consider an external time-dependent driving force acting on overdamped degrees of freedom to rectify thermal noise. For nano-systems, however, it has been pointed out that inertia terms due to finite mass should not be neglected and, actually, can help the ratchets to perform more efficiently than their overdamped companions [14]. Finite inertia typically induce in Langevin dynamics deterministic chaos that has been shown to be able to mimic the role of noise and hence to generate directed transport in the absence of external noise [15]. Here we use this effect in the different context of so-called pulsating (or effectively on-off) ratchets where the strengths of the periodic potential varies in time [10]. We consider weak thermal noise only to test for stability of the inertia induced transport — not as the source of driving. We note that in the absence of inertia, finite thermal noise *is* necessary for on-off ratchets to generate directed motion.

In this Letter we demonstrate that the system described above indeed allows for directed relative motion of the surfaces due to chaotic dynamics caused by the lateral Casimir force. The transport velocity is stable across sizeable intervals of the amplitude and frequency of surface distance oscillations and damping. The velocity scales linear with frequency across these intervals and is almost constant below a critical mean distance beyond which it drops sharply. The system exhibits multiple current reversals as function of the oscillation amplitude, mean distance and damping. The Casimir ratchet allows contact-less transmission of motion which is important since traditional lubrication is not applicable in nano-devices. This actuation mechanism should be compared to other actuation schemes as magnetomotive or capacitive (electrostatic) force transmission. The Casimir effect induced actuation has the advantage of working also for insulators and does not require any electrical contacts and/or external fields. It can also scale down effects of parasitic capacitance that reduces the efficiency of actua-

tion at high frequencies [4]. It should be mentioned that other applications of zero-point fluctuation induced (van der Waals) interactions to nano-devices have been experimentally realized already to construct ultra-low friction bearings from multiwall carbon nanotubes [16].

In the following, we consider two (on average) parallel metallic surfaces with periodic, uni-axial corrugations (along the x_1 -axis) that have distance H , see inset (a) of Fig. 1. To begin with, we assume that both surfaces are at rest with a relative lateral displacement b . Then the surface profiles can be parametrized as

$$h_1(x_1) = a \sum_{n=1}^{\infty} c_n e^{2\pi i n x_1 / \lambda_1} + \text{c.c.}, \quad (1a)$$

$$h_2(x_1) = a \sum_{n=1}^{\infty} d_n e^{2\pi i n (x_1 - b) / \lambda_2} + \text{c.c.}, \quad (1b)$$

where a is the corrugation amplitude, λ_1, λ_2 are the corrugation wave lengths, c_n, d_n are Fourier coefficients.

The Casimir energy \mathcal{E} of this configuration is the *change* of the ground state energy of the electromagnetic field due to the suppression of the tangential electric field at the surfaces. The dependence of \mathcal{E} on H and b causes macroscopic forces on the surfaces. For a varying separation H this is the normal Casimir attraction between metallic surfaces [17], modified by the corrugations. Below we will assume $H = H(t)$ to be a time-dependent distance that is kept at a fixed oscillation by an additional external force from clamping to an oscillator. In such setup, the surfaces can react freely only to the lateral force component $\mathcal{F}_{\text{lat}}(b, H) = -\partial\mathcal{E}/\partial b$. This side-ways force has been computed for sinusoidal corrugations to second order in the amplitude a , using a path integral formulation [8]. This result is readily extended to periodic profiles of arbitrary shapes as described by Eq. (1). We find that the corrugation length have to be commensurate, $\lambda_1/\lambda_2 = p/q$ with integers p, q in order to produce a finite lateral force per surface area. For the purpose of this work, it is sufficient to consider the case $p = 1$. The lateral (b -dependent) part of the Casimir energy per surface area can then be written as

$$\mathcal{E}(b) = \frac{2\hbar c a^2}{H^5} \sum_{n=1}^{\infty} \left(c_n d_{-n} e^{-2\pi i n b / \lambda_1} + \text{c.c.} \right) J\left(n \frac{H}{\lambda_1}\right) \quad (2)$$

to order a^2 . The exact form of the function J was obtained in Ref. 8 in terms of transcendental functions. For the present purpose it is sufficient to use the simplified expression

$$J(u) \simeq \frac{\pi^2}{120} (1 + 2\pi u + \gamma u^2 + 32u^4) e^{-2\pi u} \quad (3)$$

with $\gamma = 12.4133$, which is exact for both asymptotically large and small u and approximates the exact results with sufficient accuracy for all u . (The maximal deviation from the exact result is $\approx \pm 0.5\%$ around $u = 0.5$.)

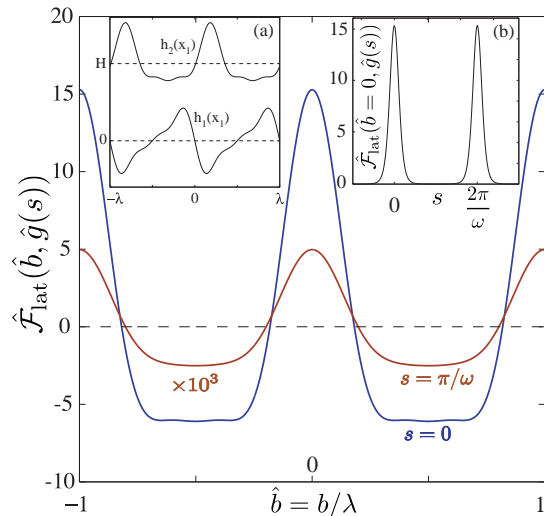


FIG. 1: The lateral Casimir force acting between the two surfaces as function of the shift \hat{b} at time $s = 0$ and half period $s = \pi/\omega$ (drawn to a larger scale by a factor 10^3) for parameters $\eta = 0.65$, $H_0 = 0.1\lambda$. Insets: (a) Surface profiles at their equilibrium position at $\hat{b} = 0.182$ (b) Periodic variation of the maximum force at $\hat{b} = 0$ with time.

The Casimir potential of Eq. (2) has two interesting properties which are useful to the construction of a ratchet. First, it decays exponentially with H , and thus can be essentially switched on and off periodically in time by oscillating H . Second, the potential is not only periodic in b but acquires asymmetry from the surface profiles at small $H \ll \lambda$ and an universal symmetric shape for $H \gg \lambda$ since the effect of higher harmonics of the surface profile is exponentially diminished [18].

The relative surface displacement $b(t)$ can be considered as a classical degree of freedom with inertia. Its equation of motion is described by Langevin dynamics of the form

$$\rho \ddot{b} + \gamma \dot{b} = \mathcal{F}_{\text{lat}}[b, H(t)] + \sqrt{2\gamma\rho T} \xi(t), \quad (4)$$

where ρ is the mass per surface area, γ the friction coefficient, T the intensity (divided by surface area) of the Gaussian noise $\xi(t)$ with zero mean and correlations $\langle \xi(t)\xi(t') \rangle = \delta(t - t')$ so that the Einstein relation is obeyed. This stochastic term describes ambient noise due to effects of temperature and pressure. (Additional contributions from thermally excited photons to the Casimir force can be neglected at surface distances well below the thermal wavelength $\hbar c/(2T)$.) The system is driven by rigid oscillations of one surface so that the distance $H(t) = H_0 g(t)$ oscillates about the mean distance H_0 with $g(t) = 1 - \eta \cos(\Omega t)$. For simplicity, we consider now equal corrugation lengths $\lambda_1 = \lambda_2 \equiv \lambda$. We define the following dimensionless variables: $\hat{b} = b/\lambda$, $s = t/\tau$ for lateral lengths and time with the typical time scale $\tau = (\lambda/a)\sqrt{\rho H_0^3/\hbar c}$ resulting from a balance between inertia and Casimir force. Hence velocities will be measured in units of $v_0 = \lambda/\tau$. There are five di-

dimensionless parameters which can be varied independently for fixed surface profiles: the damping $\hat{\gamma} = \tau\gamma$, the angular frequency $\omega = \tau\Omega$, the driving amplitude η , the scaled mean distance H_0/λ and the noise intensity $\hat{T} = (T/\hbar c)(H_0^5/a^2)$. The dimensionless equation of motion for $\hat{b}(s)$ reads

$$\ddot{\hat{b}} + \hat{\gamma}\dot{\hat{b}} = \hat{\mathcal{F}}_{\text{lat}}[\hat{b}, \hat{g}(s)] + \sqrt{2\hat{\gamma}\hat{T}}\hat{\xi}(s) \quad (5)$$

with the Casimir force

$$\hat{\mathcal{F}}_{\text{lat}}(\hat{b}, \hat{g}) = \frac{4\pi}{\hat{g}^5} \sum_{n=1}^{\infty} f_n \cos(2\pi n\hat{b}) J\left(n\hat{g}\frac{H_0}{\lambda}\right), \quad (6)$$

where we have chosen surface profiles with $c_n = i\sqrt{f_n/(2n)}$, $d_n = \sqrt{f_n/(2n)}$ with real coefficients f_n in Eq. (1), and $\hat{g}(s) = 1 - \eta \cos(\omega s)$.

We begin to analyze Eq. (5) by noting that directed transport is possible in certain parameter ranges even in the deterministic case where noise is absent. However, to probe the robustness of transport, we consider in the following primarily the limit of weak noise by choosing $\hat{T} = 10^{-3}$. In fact, it has been shown for underdamped ratchets with time-independent potentials and periodic driving that even an infinitesimal amount of noise can change the rectification from chaotic to stable [14]. To look for similar generic behavior of our pulsating ratchet, we consider a specific geometry consisting of a symmetric and a sawtooth-like surface profile corresponding to three harmonics with $f_1 = 0.0492$, $f_2 = 0.0241$, $f_3 = 0.0059$ and $f_n = 0$ for $n > 3$. Inset (a) of Fig. 1 shows these profiles in their stable position with $\hat{b} = 0.182$ that minimizes the Casimir energy. The resulting spatial variation of the Casimir force with \hat{b} is plotted in Fig. 1 for minimal ($s = 0$) and maximal ($s = \pi/\omega$) surface distance with parameters $H_0/\lambda = 0.1$, $\eta = 0.65$. It can be clearly seen that the asymmetry is reduced at larger distance where the variation of the force becomes more sinusoidal. Inset (b) shows the on-off-like time-dependence of the force amplitude at $\hat{b} = 0$ due to the oscillating surface distance.

The non-linear equation of motion of Eq. (5) has to be solved numerically. The trajectory $\hat{b}(s)$ was obtained from a second order Runge-Kutta algorithm. As initial conditions we used an equidistant distribution over the interval $[-1, 1]$ for $\hat{b}(0)$ and $\dot{\hat{b}}(0) = 0$. For each set of parameters we calculated 200 different trajectories from varying initial conditions and noise, each evolving over 4×10^3 periods $2\pi/\omega$ so that transients have decayed. The average velocity $\langle\langle v \rangle\rangle$ involves two different averages of $\dot{\hat{b}}(s)$: The first average is over initial conditions and noise for every time step, then the averaged trajectory is averaged over all discrete times of the numerical solution. For an efficient directed transport it is not sufficient to have only a finite average $\langle\langle v \rangle\rangle$. To exclude trajectories with a high number of velocity reversals, the fluctuations

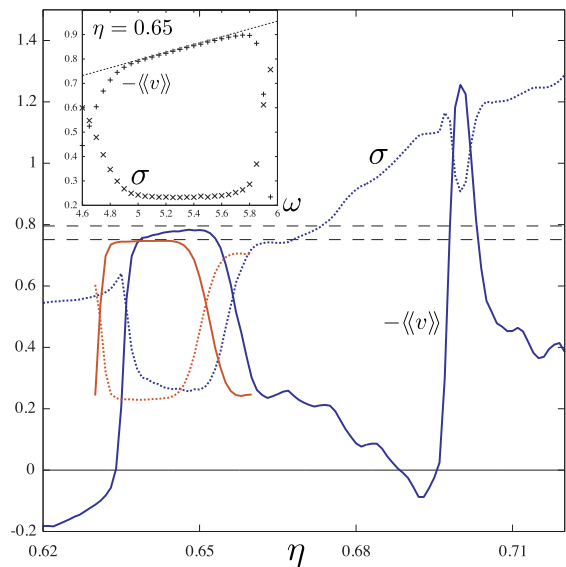


FIG. 2: Mean $\langle\langle v \rangle\rangle$ and standard deviation σ of the (negative) velocity as function of the driving amplitude η for the frequencies $\omega = 5.0$ and $\omega = 4.72$ (for the latter only the stable plateau is shown). The parameters are $H_0 = 0.1\lambda$, $\hat{\gamma} = 0.9$, $\hat{T} = 10^{-3}$. Inset: Dependence of the same quantities on frequency for fixed $\eta = 0.65$. Straight dashed lines correspond in both graphs to the velocity $\omega/(2\pi)$.

about the average velocity must be small, i.e., the variance $\sigma^2 = \langle\langle v^2 \rangle\rangle - \langle\langle v \rangle\rangle^2$ must be smaller than $\langle\langle v \rangle\rangle^2$.

Naively, one can expect directed motion of the surface profile $h_2(x_1)$ into the positive x_1 -direction ($\dot{\hat{b}} < 0$) since the Casimir force in Fig. 1 is asymmetric with negative values lasting for longer time than positive ones. However, the actual behavior is more complicated due to chaotic dynamics. Fig. 2 shows the dependence of the average velocity and its standard deviation σ on the driving amplitude η and frequency ω for $H_0 = 0.1\lambda$, $\hat{\gamma} = 0.9$. For a fixed frequency there is an optimal interval of driving amplitudes across which the average velocity is almost constant with $\langle\langle v \rangle\rangle \simeq -\omega/(2\pi)$. Small deviations from the latter value result from noise as we have checked by studying the dynamics at $\hat{T} = 0$. At higher driving amplitudes we observe a second narrower interval with maximal $\langle\langle v \rangle\rangle$ which is more strongly reduced and smeared out from its deterministic value $-2 \times \omega/(2\pi)$ by noise. At the plateaus of constant velocity the standard deviation σ is substantially reduced, rendering transport efficient. Outside the plateaus velocity reversals occur and σ increases linearly with η . For fixed amplitude η , the average velocity is stable at the value $-\omega/(2\pi)$ over a sizeable frequency range (see inset of Fig. 2).

In order to understand the observed behavior we have analyzed the dynamics in the three dimensional extended phase space. There attractors of the long-time dynamics can be identified from Poincaré sections using the period $2\pi/\omega$ of the surface oscillation as stroboscopic time. To obtain a compact section, the trajectory is folded period-

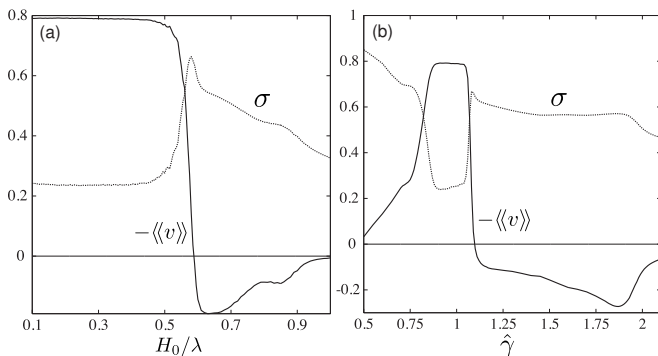


FIG. 3: Mean $\langle\langle v \rangle\rangle$ and standard deviation σ of the (negative) velocity as function of (a) the mean plate distance H_0 for $\hat{\gamma} = 0.9$ and (b) damping $\hat{\gamma}$ for $H_0 = 0.1\lambda$. The other parameters are $\eta = 0.65$, $\omega = 5.0$, $\hat{T} = 10^{-3}$.

ically in x_1 on one period of the Casimir potential. From these sections we can distinguish between periodic and chaotic orbits. As a start, we consider the deterministic limit with $\hat{T} = 0$. The plateaus around $\eta = 0.65$ and $\eta = 0.7$ result both from periodic orbits of period one, corresponding to a single point in the Poincaré section. On the right (downward) edges of the first plateaus we have observed period doubling, i.e., a periodic attractor with period two. Upon a further increase of η , chaotic orbits dominate the motion. Hence the system exhibits a period-doubling route to chaos with enhanced velocity fluctuations. The findings apply basically also to weak noise ($\hat{T} = 10^{-3}$) but the sharp points of the periodic attractors in the Poincaré sections are smeared out leading to a decreased $\langle\langle v \rangle\rangle$. The transition from chaotic to periodic dynamics at the beginning of the rising edge of the plateaus is accompanied by a velocity reversal. This is consistent with the earlier observation for non-pulsating potentials that velocity reversals are due to a bifurcation from chaotic to periodic dynamics [15].

The amplitude of the Casimir potential can be tuned by varying the mean distance H_0 . From Fig. 3(a) we see that the dynamics show a sharp transition at a critical H_0/λ from efficient transport with large $\langle\langle v \rangle\rangle$ and small σ to chaotic dynamics with vanishing velocity. The transition is accompanied by a velocity reversal and peaked velocity fluctuations. Interestingly, below the transition $\langle\langle v \rangle\rangle$ is almost constant independently of H_0/λ . The observed transport behavior is also stable against a change of effective damping $\hat{\gamma}$ as shown in Fig. 3(b). Whereas fluctuations increase with decreasing $\hat{\gamma}$, there is a stable plateau of constant average velocity across which fluctuations are diminished. In the deterministic limit, we have also observed additional plateaus with inverted and doubled average velocity by varying $\hat{\gamma}$ and η . Remnants of a second plateau around $\hat{\gamma} = 1.9$, washed out by noise, can be seen in Fig. 3(b).

Finally, let us estimate typical velocities $v_0 = \lambda/\tau$. With the typical lengths $H_0 = 0.1\mu\text{m}$, $a = 10\text{nm}$ realized in recent Casimir force measurements [9] and an

area mass density of $\rho = 10\text{g/m}^2$ for silicon plates with a thickness of a few microns, one obtains $v_0 = \sqrt{\hbar c a^2 / \rho H_0^5} \approx 5.5\text{mm/s}$. The actual average velocity $v_0\omega/2\pi$ is of the same order for the frequencies studied above. For $\lambda = 1\mu\text{m}$, the time scale is $\tau = \lambda/v_0 \approx 10^{-4}\text{s}$ leading to driving frequencies and damping rates in the kHz range for the parameters considered here.

Our results show that Casimir interactions offer novel contact-less translational actuation schemes for nanomechanical systems. Similar ratchet-like effects are expected between objects of different shapes as, e.g., periodically structured cylinders, inducing rotational motion. The use of fluctuation forces appear also promising to move nano-sized objects immersed in a liquid where electrostatic actuation is not possible. Another application is the separation and detection of particles of differing mass adsorbed to the surfaces. For surfaces oscillating at very high frequencies additional interesting phenomena related to the dynamical Casimir effect occur [19], leading to the emission of photons that could contribute to ratchet-like effects as well.

I acknowledge useful discussions with R. Golestanian and M. Kardar.

-
- [1] E. Buks and M. L. Roukes, *Europhys. Lett.* **54**, 220 (2001).
 - [2] H. B. Chan, V. A. Aksyuk, R. N. Kleiman, D. J. Bishop, and F. Capasso, *Science* **291**, 1941 (2001).
 - [3] H. B. Chan, V. A. Aksyuk, R. N. Kleiman, D. J. Bishop, and F. Capasso, *Phys. Rev. Lett.* **87**, 211801 (2001).
 - [4] E. Buks and M. L. Roukes, *Phys. Rev. B* **63**, 033402 (2001).
 - [5] E. Buks and M. L. Roukes, *Nature* **419**, 119 (2002).
 - [6] O. Kenneth, I. Klich, A. Mann, and M. Revzen, *Phys. Rev. Lett.* **89** (2002).
 - [7] T. Emig, A. Hanke, R. Golestanian, and M. Kardar, *Phys. Rev. Lett.* **87**, 260402 (2001).
 - [8] T. Emig, A. Hanke, R. Golestanian, and M. Kardar, *Phys. Rev. A* **67** (2003).
 - [9] F. Chen, U. Mohideen, G. L. Klimchitskaya, and V. M. Mostepanenko, *Phys. Rev. Lett.* **88** (2002).
 - [10] P. Reimann, *Phys. Rep.* **361**, 57 (2002).
 - [11] F. Jülicher, A. Ajdari, and J. Prost, *Rev. Mod. Phys.* **69**, 1269 (1997).
 - [12] R. D. Astumian and I. Derenyi, *Eur. Biophys. J.* **27**, 474 (1998).
 - [13] C. C. de Souza Silva, J. Van de Vondel, M. Morelle, and V. V. Moshchalkov, *Nature* **440**, 651 (2006).
 - [14] F. Marchesoni, S. Savel'ev, and F. Nori, *Phys. Rev. E* **73**, 021102 (2006).
 - [15] J. L. Mateos, *Phys. Rev. Lett.* **84**, 258 (2000).
 - [16] J. Cumings and A. Zettl, *Science* **289**, 602 (2000).
 - [17] H. B. G. Casimir, *Kon. Ned. Akad. Wetensch. Proc.* **51**, 793 (1948).
 - [18] R. Buscher and T. Emig, *Phys. Rev. Lett.* **94**, 133901 (2005).
 - [19] R. Golestanian and M. Kardar, *Phys. Rev. Lett.* **78**, 3421 (1997).